



AIAA 99-0945

**A New Heat Transfer Capability
for Application in Hypersonic
Flow Using Multiple Schmidt-
Boelter Gages**

W. R. Hawkins, C. T. Kidd, and J. S. Carter
Sverdrup Technology, Inc., AEDC Group
Arnold Engineering Development Center
Arnold Air Force Base, Tennessee 37389

19991130 104

**37th AIAA Aersopace Sciences
Meeting & Exhibit
January 11-14, 1999 / Reno, NV**

A New Heat Transfer Capability for Application in Hypersonic Flow Using Multiple Schmidt-Boelter Gages*

*W. R. Hawkins,[†] C. T. Kidd, and J. S. Carter
Sverdrup Technology, Inc., AEDC Group
Arnold Engineering Development Center
Arnold Air Force Base, TN 37389*

Abstract

Heat-transfer measurements were made on a complex scaled wind tunnel model containing 400 miniature discrete sensors in Hypersonic Wind Tunnels B and C at the Arnold Engineering Development Center (AEDC). This test program was significant for a number of reasons which, when combined, have led to the development of a new test capability at the AEDC. First and foremost is the large number of simultaneous thermal measurements made on the wind tunnel test model. The large number of simultaneous measurements on a single test model was primarily driven by the customer's desire to conduct the test program in the most cost-effective manner. This request was translated into a system to obtain high-quality test data points in the least amount of air-on time and to make heat-transfer measurements on all surfaces of a very complex model. The measurements were made on relatively flat surfaces, wing leading edges, and thin tip fin leading edges; multiple measurements were made on a wide variety of unconventional control surfaces and appendages. Simultaneous measurements on the wide variety of surfaces required the selection of a sensor which was highly sensitive, small, and could be contoured to small local surface radii. The sensor chosen for these measurements was the Schmidt-Boelter gage. The capability to calibrate Schmidt-Boelter gages and compare a National Institute of Standards and Technology (NIST)-traceable and certified standard is one reason this sensor was used for all of the measurements. Since each gage needs the measurement of two thermal parameters to obtain the required measurement parameter, the simultaneous measurement of 800 thermal parameters was

required. The previous data acquisition system in these hypersonic wind tunnels at the AEDC was capable of measuring outputs for only 112 Schmidt-Boelter gages simultaneously. Therefore, a new robust and mobile data acquisition system configured specifically to accommodate the large number of measurement parameters for this test program was designed and fabricated. The cost-effective test techniques, the Schmidt-Boelter gage, the new data acquisition system, and the overall data quality achieved in this significant test program will be described and emphasized in the paper.

Nomenclature

- C_1 Gage calibration scale factor, Btu/ft²-sec/mv
- C_2 Experimental constant to determine temperature difference between gage surface and wafer back surface, °R/mv
- E Installed S-B gage output voltage, mv
- E_0 Calibration S-B gage output voltage, mv
- H_{TR} Heat-transfer coefficient based on recovery temperature, Btu/ft²-sec-°R
- K_1 Thermal conductivity of parallel wall slab, Btu/ft-sec-°R
- k Thermal conductivity of wafer, Btu/ft-sec-°R
- l S-B gage slab thickness, ft
- N Number of wire turns on the wafer
- q S-B gage measured heat-transfer rate, Btu/ft²-sec
- q_0 Laboratory calibration input heat flux, Btu/ft²-sec

* The research reported herein was performed by the Arnold Engineering Development Center (AEDC), Air Force Materiel Command. Work and analysis for this research were performed by personnel of Sverdrup Technology, Inc., AEDC Group, technical services contractor for AEDC. Further reproduction is authorized to satisfy needs of the U. S. Government.

[†] Senior Member, AIAA.

Approved for public release; distribution unlimited.

- T_B Measured temperature at back surface of S-B gage wafer, °R
- T_C S-B gage lower (cold) surface temperature, °R (see Fig. 6)
- T_D Difference between S-B measured and actual outer gage surface temperature, °R
- T_H S-B gage top surface temperature, °R (see Fig. 6)
- T_R Assumed recovery temperature, °R
- T_W Model outer surface temperature, °R
- ΔT Temperature difference between S-B gage wafer top and lower surface, $\Delta T = T_H - T_C$, °R
- t Time, seconds
- x Depth into parallel wall slab, in.
- σ Absolute Seebeck coefficient of the combined S-B thermoelements, (mv/°R)

1.0 Introduction

Development of hypersonic flight systems usually requires a large volume of high-quality experimental ground test data which are used to predict flight performance and validate supporting analytical codes. In the development of past complex hypersonic flight vehicles (e.g., U.S. Space Shuttle), the Arnold Engineering Development Center (AEDC) made significant contributions with the acquisition of substantial quantities of high-quality experimental supersonic and hypersonic wind tunnel data. In recent years, significant improvements have been made in experimental methods, both in the quality and quantity of test data obtained during wind tunnel test entries. With today's restricted budgets, increased cost of wind tunnel test time, and competition from other facilities, it is necessary to provide the customer the best possible value for his test budget dollar. This is accomplished, in part, at the AEDC with detailed pre-test planning for cost-effective testing. The continual development of new measurement sensors, coupled with the design and implementation of significantly improved data acquisition capabilities, makes it possible to obtain more high-quality experimental wind tunnel data in less tunnel air-on time. The higher productivity capabilities are realized through

significantly improved data acquisition and processing, better sensors, and detailed, innovative test planning. The purpose of this paper is to: (1) Describe the highly sensitive miniature Schmidt-Boelter gage and its calibration and measurement application in heat-transfer measurements in complex flow environments on unconventional model surfaces such as small radii wing leading edges and thin tip fin leading edges, and (2) Describe a new robust and mobile data acquisition system designed, fabricated, and configured specifically to accommodate a large number of measurement parameters.

The Schmidt-Boelter gage is a sensor which has a high sensitivity, small size, and is contourable to small local surface radii. Sensors of this type were fabricated in miniature (0.062 and 0.125) and conventional (0.187-in.) diameter sizes. Some of the gages were fabricated in lengths less than 0.10 in. in order to make measurements on some of the thin model surfaces. The Schmidt-Boelter gage features simultaneous measurements of surface heat flux and temperature in order to provide a local heat-transfer coefficient at each of the sensor locations on the model body.

A related requirement was a new data system with the ability to measure low output signals from the sensors. The test model experienced wide variations in aerodynamic heating from windward and leeward model surfaces as the model was subjected to varying angles of attack during the test program conducted at hypersonic flow Mach numbers of 6, 8, and 10. An unusually high quantity of tabulated data and plots was available within minutes of each model injection into the tunnel flow.

Testing of the HOPE (H-II Orbiting Plane) configuration was executed in the fall of 1996 and winter of 1997 at the AEDC. Aerothermal heat-transfer data were obtained simultaneously at 400 different locations on a scaled HOPE model using a newly developed modular multiplexed data acquisition system. A decision was made early in the test program planning to use only Schmidt-Boelter gages^{1,2} to make these aerodynamic heat-transfer measurements. One of the many reasons for the selection of Schmidt-Boelter gages was the sensor's ability to be calibrated to high accuracy (± 1.7

percent uncertainty) with standards traceable to the National Institute of Standards and Technology (NIST). The measurement methodology of the exclusive use of direct-reading Schmidt-Boelter gages will be explained in a later section of this paper. The success of this test program established the miniature Schmidt-Boelter gage as the AEDC sensor of choice in similar measurement applications.

2.0 Facility Description

AEDC Hypersonic Wind Tunnels B and C, (Fig. 1), are large closed-circuit continuous flow, variable density wind tunnels with 50-in.-diam (1.3 m) test sections. Axisymmetric contoured nozzles provide free-stream Mach numbers of 6 and 8 in Tunnel B and 10 in Tunnel C. These tunnels operate over a stagnation pressure range of 50 to 300 psia at Mach 6, 100 to 900 psia at Mach 8, and 200 to 2000 psia at Mach 10. Stagnation temperatures up to 1440°F (768°C) are obtained through the use of natural gas-fired combustion heaters in series with an electric resistance heater. These tunnels are equipped with a model injection system which permits model removal from the tunnel while the tunnel remains in operation. The injection system permits precision control of model flow immersion time and model wall initial conditions. An additional advantage of the injection system is to permit model accessibility for rapid configuration changes while the tunnel remains in operation. The injection tank also contains an air cooling system to assist in regaining isothermal model-wall initial conditions. Tunnel B and the model injection system are also illustrated in Fig.1, and a more detailed description of these tunnels may be found in Ref. 3.

3.0 Test Article and Test Conditions

The test article (Figs. 2 and 3) was a scaled model of the HOPE unmanned, winged space vehicle which contained a variety of instrumented control surfaces. Some of these control surfaces were relatively flat while others had thin cross-sectional areas with very small radii of curvature, as shown in Fig. 4. These features made the selection of heat-transfer sensors quite difficult. Measurement of aerodynamic heat transfer on these types

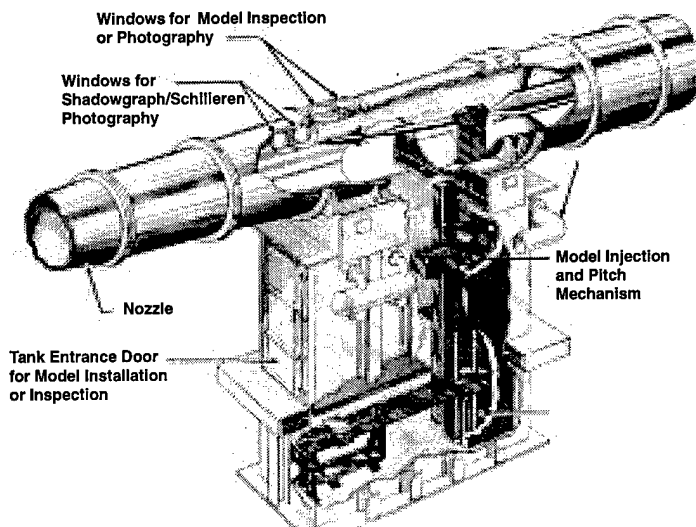


Fig. 1. AEDC Hypersonic Wind Tunnels B and C.

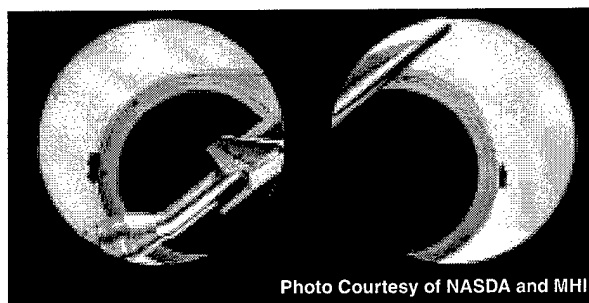


Fig. 2. HOPE Wind Tunnel model installed in AEDC Hypersonic Wind Tunnel B.

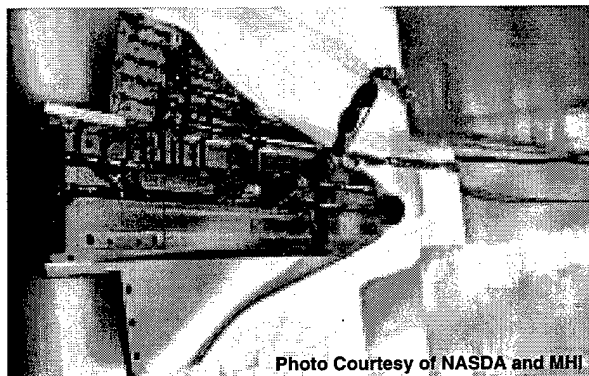


Fig. 3. HOPE Wind Tunnel model lower assembly.

of surfaces has always been difficult,⁴ and previous measurements⁵ contained error as a result of heat conduction. The model was designed to accommodate 400 Schmidt-Boelter heat-transfer gages. The lead wires from each gage consisted of one twisted pair copper for heat flux signal and one duplex pair Type-J thermocouple for the surface temperature measurement. These wires were

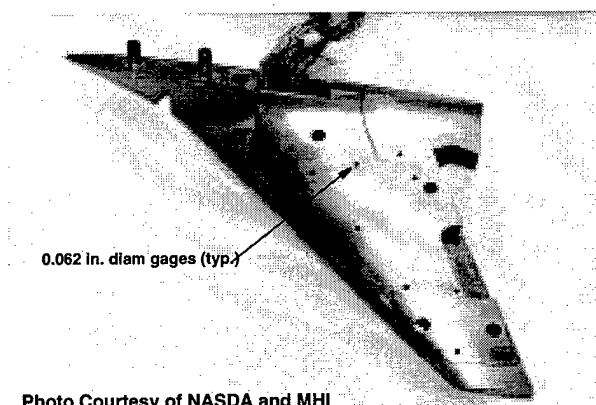


Photo Courtesy of NASDA and MHI

Fig. 4. HOPE model tip fin control surface instrumentation.

routed in four main cable arrangements (Fig. 5) and bound together in the attaching hardware downstream to form a continuous cable to the new data acquisition system.

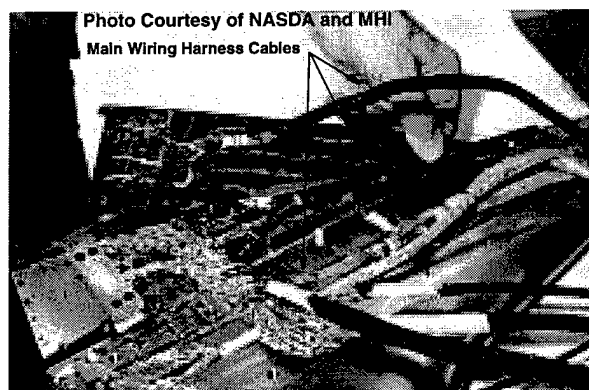


Photo Courtesy of NASDA and MHI

Fig. 5. HOPE model instrumentation buildup.

The test article was injected into the flow at uniform temperature (nominally 100°F) at pre-selected model attitude angles of alpha and beta. Mach number effects at 6 and 8 in Tunnel B and Mach 10 in Tunnel C were each evaluated for several model configurations. Data acquisition was initiated within 0.5 sec after attaining tunnel centerline.

4.0 Discussion of Measurement Methodology

Peak aerodynamic heating on most high-speed flight vehicles occurs on nosetips, wing leading edges, and tip fins. It is reasonable that designers of this class of vehicle need ground test facility heat-transfer data to quantify aerodynamic heating in these regions. The challenge is that wind tunnel models are generally small relative to full-scale

vehicles, resulting in nosetips and leading edge surface radii as small as 0.015 in. The usual approach to providing data that define aerodynamic heating for scaled models of complex hypersonic flight vehicles in wind tunnels is to make measurements on individual sections of the model rather than the entire body. Reasons for this are simple and include the following:

1. It is difficult to instrument entire models if they contain small radius of curvature areas such as wing leading edges, tip fins, nosetips, and multiple control surfaces.

2. Instrumentation of the entire model for effective coverage often would require several hundred measurements to be made simultaneously, and therefore require many more data acquisition channels than are currently available at most wind tunnel facilities.

3. Heat flux levels over the entire model vary greatly, especially when the test model is subjected to a wide angle-of-attack range at variable test conditions.

4. Aerodynamic heating on surfaces such as relatively flat wings, body, and fuselage are more easily measured with common discrete methods such as thin-skin thermocouples,^{5,6} Gardon gages,^{7,8} coaxial thermocouples,^{9,10} or conventional Schmidt-Boelter gages.^{1,2}

5. Areas such as wing leading edges and tip fins have been and remain more difficult to model and measure because of their small radius of curvature which is not readily amenable to measurement with common methods.

Conventional heat-transfer sensors do not adapt well to these small radius regions. Measurement of heat transfer in these areas has always been difficult, and the search for more accurate and effective methods of measurement has been a continual and difficult quest. Schmidt-Boelter gages were best suited to the heat-transfer measurements required on this complex aerodynamic model because the Schmidt-Boelter gage may be contoured in one axis of symmetry. Therefore, these small sensors could be placed in areas of

very small radius of curvature if the perpendicular axis is nearly straight. Medtherm Corp. of Huntsville, AL, provided approximately one-half of the heat flux sensors that were designed specifically for this application. The sensors provided by Medtherm were small diameter (0.062 in. or 0.159 cm) Schmidt-Boelter gages that were primarily used on the wing leading edges, tip fins, and other areas requiring small radii of curvature. The remaining one-half of the Schmidt-Boelter gages were designed, fabricated, calibrated, and installed by AEDC personnel. A schematic depicting a typical Schmidt-Boelter gage fabricated at AEDC is shown in Fig. 6. These gages were 0.125 in. (0.318 cm) and 0.187 in. (0.476-cm) diameter and are generally considered small enough for the majority of aerodynamic heating tests in the AEDC hypersonic wind tunnels.

4.1 Principle of Operation

It is understood that operation and data reduction principles of the Schmidt-Boelter gage are documented in reference materials; however, it is the author's opinion that these principles should be presented in this paper for completeness. The principle of operation of the Schmidt-Boelter gage can readily and correctly be divided into two distinctly

different physical principles. These are the thermal and thermoelectric functions. There are valid reasons for separating the individual functions, and for a complete understanding of gage operation, detailed descriptions of both the thermal and thermoelectric principles are given in Ref. 2.

For the purposes of this paper, the Schmidt-Boelter gage concept is adequately represented by Fig. 6. From a thermal perspective, the gage operates on the principle of axial heat conduction. It can be shown that for a constant heat flux, \dot{q} , on the surface, a constant temperature differential, ΔT , is developed between the top and bottom surfaces of an electrically insulating wafer that is in ideal thermal contact with another material which effectively serves as a heat sink. The temperature differential, ΔT , is a measurement of the difference in temperatures at the top surface, T_H , and the bottom surface, T_C , of the wafer; i.e., $\Delta T = T_H - T_C$. A differential thermocouple measuring this temperature difference will have an output signal, E_0 , which is proportional to the input heat flux, \dot{q} . The thermoelectric function of the gage is achieved by winding a small diameter bare constantan wire around a wafer of an electrically insulating material (thermal resistance layer). One-half of the wire/wafer assembly is then electroplated with a material ther-

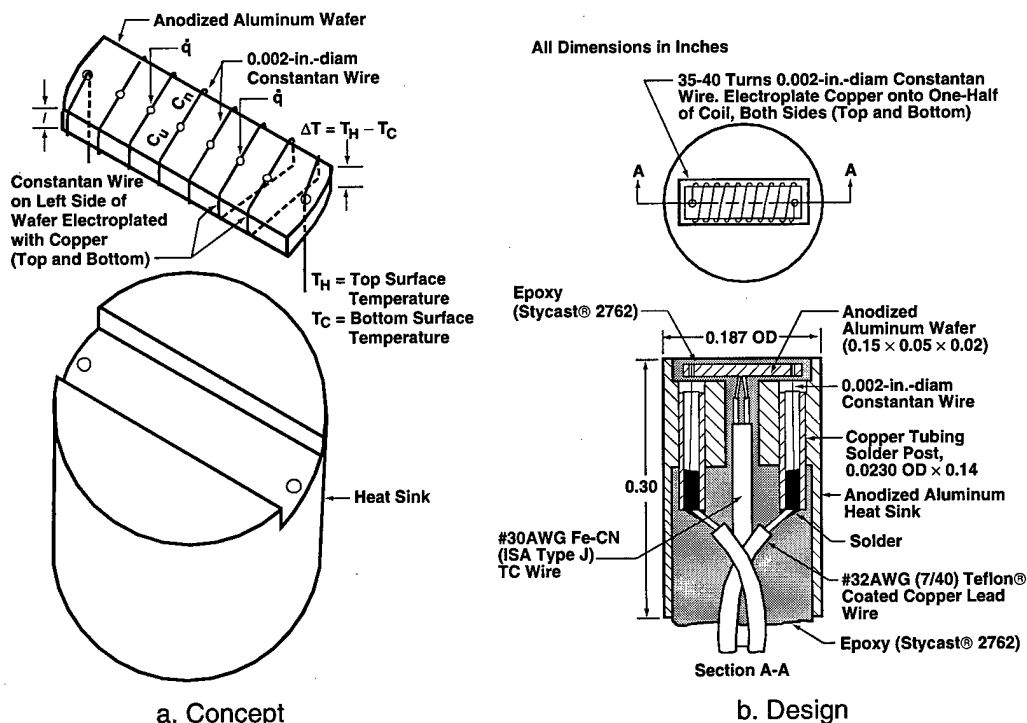


Fig. 6. AEDC Schmidt-Boelter gage.

moelectrically compatible with constantan thermocouple wire. Boelter used silver as the plating material in his initial gage, but most manufacturers now use copper. This electrical configuration effectively creates a series combination of copper-constantan differential thermocouples with the hot junctions at a temperature, T_H , on the top surface of the wafer and the cold junctions at a temperature, T_C , on the bottom surface. This series combination of differential thermocouples is called a thermopile. The output signal from the gage is directly proportional to the number of windings of the constantan wire around the insulating wafer. The output signal can be represented by the following equation:

$$E_0 = N \sigma^* (T_H - T_C) = N \sigma^* \Delta T \quad (1)$$

where N is the number of turns of constantan wire around the wafer and σ is the absolute Seebeck coefficient¹¹ of the series combination of thermoelements.

A mathematical model which is often used to simulate a Schmidt-Boelter gage is the parallel wall slab backed by a semi-infinite solid. The geometric representation of this math model is shown in Fig. 7. Exact solutions for the transient temperature history at any axial station, x , on or into the parallel wall slab are available in several heat conduction texts or reports.^{12,13} These temperature histories or combinations of temperature difference histories are easily programmed for repetitive calculations on a digital computer. However, there are assumptions which must be made to make gage performance calculations using exact solutions. The gage is assumed to have only two components,

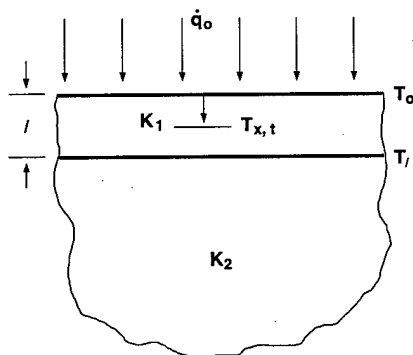


Fig. 7. Parallel wall slab backed by semi-infinite solid.

which can be two different materials. These are the parallel wall slab and a backing or heat sinking material. Heat flux sensitivity is determined by calculating the temperature difference, $T_H - T_C = \Delta T$, between the top and bottom surfaces of the parallel wall slab. The steady-state solution to the problem is given by:

$$\Delta T = \frac{q_0}{K_1} l \quad (2)$$

where K_1 and l are the thermal conductivity and thickness of the slab, respectively, and q_0 is the heat flux input. Also, the l in Eq. (2) represents the same ΔT shown in Eq. (1). The derivation of Eq. (2) can be found in several papers or texts, including Ref. 1.

While Eqs. (1) and (2) are useful for showing how the Schmidt-Boelter gage develops its output, many actual gages are composed of several different materials due to the requirements of the applications for which they are intended. These often include environmental considerations such as pressure, temperature, humidity, etc. This causes the thermal model of the actual gage to be much different from the simple model. Finite element analysis (FEA) heat conduction codes have been successfully employed to predict the thermal response of the gages to good accuracy. Results of thermal analyses to define the heat conduction paths in the thermal model of gages used in wind tunnel tests at the AEDC are presented in Refs. 1, 2, and 14.

4.2 Data Reduction

Since the Schmidt-Boelter gage is a discrete transducer featuring a self-generating output directly proportional to the heat flux incident on its surface, the steady-state output signal of the thermopile is proportional to the incident heat flux at the surface, and a temperature difference is developed between parallel planes inside the gage shown in Eqs. (1) and (2). The constant terms in these equations can be grouped together such that the heat flux on the gage can be related to the output from the differential thermocouple series combination as:

$$\dot{q} = C_1 E \quad (3)$$

where C_1 is the gage calibration scale factor that is determined from the experimental laboratory calibration.

The determination of the local heat-transfer coefficient requires an effective gage surface temperature, T_w , as well as the heat flux given by Eq. (3). Since actual measurement of the surface temperature is difficult, a thermocouple is attached to the back surface of the wafer as shown in Fig. 6. The Type-J thermocouple provides a temperature measurement of the wafer back surface which is designated as T_B . The temperature difference, T_D , between the measured gage temperature and surface temperature is defined as:

$$T_D = C_2 * E \quad (4)$$

where C_2 is an experimentally determined constant which is used to calculate the difference in the gage surface temperature and the temperature measured by the thermocouple located at the back surface of the wafer based on the gage output, E .¹ The effective surface temperature, T_w , of the Schmidt-Boelter gage is then given by:

$$T_w = T_B + T_D \quad (5)$$

The heat-transfer coefficient may then be computed as:

$$h_{TR} = \dot{q} / (T_R - T_w) \quad (6)$$

where T_R is a suitable recovery temperature. A complete discussion of recovery temperatures is included in Ref. 15.

4.3 Laboratory Calibration of Schmidt-Boelter Gages

Schmidt-Boelter gages were calibrated in the AEDC Aerothermodynamics Measurements Laboratory (ATMLab). The heat source is a nine-unit 1-KW tungsten filament lamp bank which provides uniform heat flux varying from 0.5 to 10 Btu/ft²-sec over a surface area measuring 4 in. by 1.5 in.¹ Outputs from up to 24 sensors are routed to the inputs of Preston 8300 XWB instrumentation

amplifiers. These amplifiers provide gain up to 15,000 using analog filtering. Amplifier outputs are routed to the inputs of a Preston GMAD3A-15B multiplexed 15-bit analog-to-digital converter which is operated in the burst mode triggered by the computer (DEC PDP 11/73) real-time clock. A calibration through the data system using National Institute of Standards and Technology (NIST)-traceable millivolt standards is performed at the beginning of each day the system is used. Sample calibrations are shown in Fig. 8.

It has been determined by a statistical analysis that the data system adds an uncertainty of ± 0.5 percent to the experimental calibrations. A detailed description of the ATMLab laboratory data acquisition system is given in Ref. 16. Up to nineteen gages can be calibrated simultaneously using as a reference three heat flux standard 0.187-in.-diam Schmidt-Boelter gages made by Medtherm Corp. These transfer standard gages are calibrated at the NIST Optical Technology Division Physics Lab using a Variable Temperature Blackbody (VTBB) as the heat source. Calibrations of the transfer standard gages are certified to be accurate to ± 1.7 -percent deviation over a range of heat flux up to 10 W/cm² (8.81 Btu/ft²-sec). Three transfer standard gages are used over a time period up to twelve months and are then replaced with another standards group calibrated by NIST in the same manner. Experimental procedures followed by NIST in the calibration of the transfer standard gages are documented in a technical paper published in Nov. 1997.¹⁷ The calibration heat flux level is determined by taking the average of the indicated heat flux from the three transfer standard gages over a common time interval. Measured heat flux from the

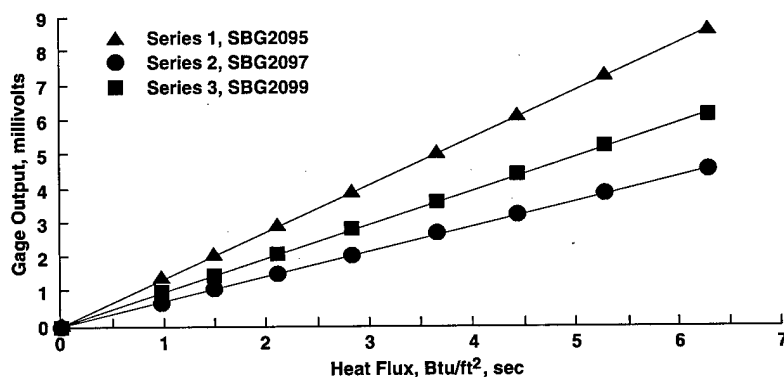


Fig. 8. AEDC Schmidt-Boelter sample calibrations.

three transfer standard gages is normally within 1-percent deviation. The output in millivolts from each of the test gages is measured over the same time interval over which the individual outputs of the transfer standard gages are measured. The calibration scale factor (Btu/ft²-sec/mv) for each gage is calculated by a straight line curve fit through three data points obtained at three different heat flux levels plus zero. Of course, the uncertainties quoted above only apply to the heat flux calibration, and not to the measurements of heat transfer coefficients. The gage surface temperature is required in the calculation of heat-transfer coefficients, and this measurement is made with special-grade thermocouple wire whose uncertainties are listed in the ASTM manual on the Use of Thermocouples in Temperature Measurement.¹¹

4.4 Application Uncertainty

The uncertainties of the final measurements were estimated using methodology contained in Ref. 18 and are a combination of bias and precision errors. Typical calibration results are shown in

Fig. 8. The uncertainties of the wind tunnel test conditions at the 95-percent confidence level for the systems used during the test are provided in Table 1 and were estimated from the tunnel calibration data and the uncertainty of the tunnel instrumentation. Propagation of the bias and precision errors of the calculated parameters of interest based on measured data are shown in Table 2. Calibrations traceable to the National Institute of Standards and Technology are available for all instrumentation and associated systems. In general the miniature Schmidt-Boelter gages demonstrated precision and bias uncertainties approaching that of a conventional gage (± 5.0 percent). Data acquisition and instrumentation calibrations are performed daily as outlined in the previous section to ensure calibration criteria are maintained.

5.0 Multiplexing System Functional Description

5.1 Requirements

The previous Tunnel A/B/C multiplexing data acquisition system was capable of simultaneous

Table 1. Schmidt-Boelter Gage Calibration Uncertainties

Parameter Description	Precision Limit (S)			Bias Limit (B)		Uncertainty (B+195°S)		Range	Type of Measuring Device	Type of Recording Device	Method of System Calibration
	Percent of Reading	Unit of Measurement	Degrees of Freedom	Percent of Reading	Unit of Measurement	Percent of Reading	Unit of Measurement				
Schmidt-Boelter Gage Heat Flux q , Btu/ft ² -sec	0.5	Btu/ft ² -sec	>30	1.7	Btu/ft ² -sec	2.2	Btu/ft ² -sec	0.5 -10 Btu/ft ² -sec	S-B reference gage	Digital Data Acquisition System	Application of multiple heat flux levels using 3 NIST calibrated secondary standards
Schmidt-Boelter gage T_H , T_D Temperature Deg R	0.5	deg R	>30	0.40%	deg R	0.9	2 deg R	490-960 deg R	Iron-Constantan Thermocouples	Digital Thermometer and micro-processor averaged	Thermocouple verification NIST conformity/voltage substitution calibration

Table 2. Schmidt-Boelter Gage Application Uncertainties

Parameter Description	Precision Limit (S)			Bias Limit (B)		Uncertainty (B+195°S)		Range	Type of Measuring Device	Type of Recording Device	Method of System Calibration
	Percent of Reading	Unit of Measurement	Degrees of Freedom	Percent of Reading	Unit of Measurement	Percent of Reading	Unit of Measurement				
Schmidt-Boelter Gage Heat Flux q , Btu/ft ² -sec	2.5	Btu/ft ² -sec	>30		0+	5.0		0.5 -10 Btu/ft ² -sec	S-B reference gage	Digital Data Acquisition System	In-place check of gage heat flux level using calibrated radiant heat source
Schmidt-Boelter gage T_H , T_D Temperature Deg R		1 deg R	>30		2 deg R		4 deg R	490-960 deg R	Iron-Constantan Thermocouples	Digital Thermometer and micro-processor averaged	Thermocouple verification NIST conformity/voltage substitution calibration

acquisition of 112 Schmidt-Boelter gages and a system upgrade was required to measure 400 Schmidt-Boelter gages in the same manner. In order to constrain costs and maintain schedules, the guidelines below were followed to select the appropriate upgrade strategy:

- Minimize changes to the existing tunnel data system hardware.
- Minimize data system software changes.
- Use existing data reduction equations.

PC-based and several off-the-shelf data systems were evaluated, but each proved too slow, too expensive or too inaccurate. It was determined that enhancement of the current data system would provide the best quality data and minimize software development costs.

The newly designed system interfaced the sensor signals to the existing data system using electronically scanned pressure (ESP) control wiring. An ESP is a device that directs information from multiple pressure sensors to one data system input amplifier. The control wiring manipulates heat flux sensor signals as well as pressure data with additional signal wiring and multiplexing hardware. Multiplexing signals in this manner permits a large number of sensors to be measured by a single data system amplifier. The new system was constructed to provide the necessary number of input channels without modifications to the existing data acquisition hardware.

5.2 System Design

The previous facility data system was capable of 48-channel addressing of ten ESP modules. This permitted the measurement of 480 pressure inputs. The redesign increased the address range to 64 channels and connected 14 additional amplifiers in order to accommodate 800 or more test article heat flux parameters. Analysis of data system timing and processing capability was also initiated. Data acquisition, display, and storage rates in excess of 16 samples a second for each heat gage signal were obtained. Each 64-channel multiplexing circuit output connects to a data system amplifier as shown in the attached schematic (Fig. 9).

It was determined that a combination of the following characteristics and functions provided the optimum accuracy.

1. The shortest possible sensor leads were used to minimize impedance mismatch and cabling costs.
2. The leads from the sensor to the system input were twisted to minimize noise pickup.
3. Isothermal inputs were maintained for the signal inputs to prevent errors in the thermocouple readings.
4. The capability to accurately measure floating (ungrounded) signals or grounded signals was provided.
5. On-card jumpers provided flexibility in setting local amplification and grounded/ungrounded gage type.

Figure 9 shows the connection for each thermocouple signal of 62 Schmidt-Boelter heat-transfer gages. The connection for each heat flux sensor is identical, except that no reference temperature measurement is needed. The circuitry for both thermocouple and heat flux sensor is contained in a single chassis. This arrangement permits both signals from a heat-transfer gage to be connected in the same physical area. Also, the two outputs are measured within one μ sec of each other.

5.3 Fabrication

The system is installed in a standard 19-in. portable instrument rack (Fig. 10) in order to simplify transportation between test facilities. One important feature of the instrument rack is that equipment can be mounted in the front or the back. In addition to the 7-multiplexer chassis and system controller, a pair of video monitors, a precision voltage source, and a storage drawer were mounted in the rack. The rack was connected to the test article through the 1600 sensor leads, to the ESP System via six address lines, and finally to the data system through 14 analog outputs and a video feed. The system includes the capability for local calibration and checkout of the equipment.

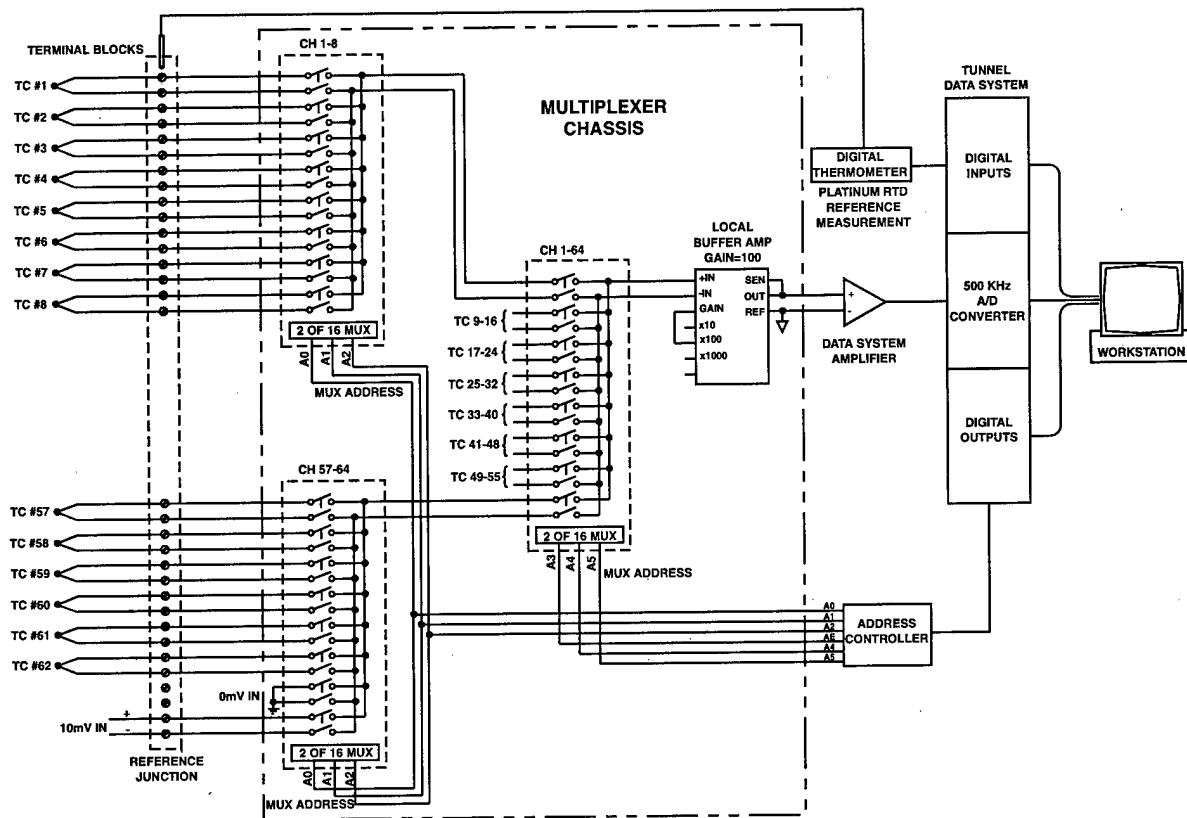


Fig. 9. Multiplexer circuit schematic.

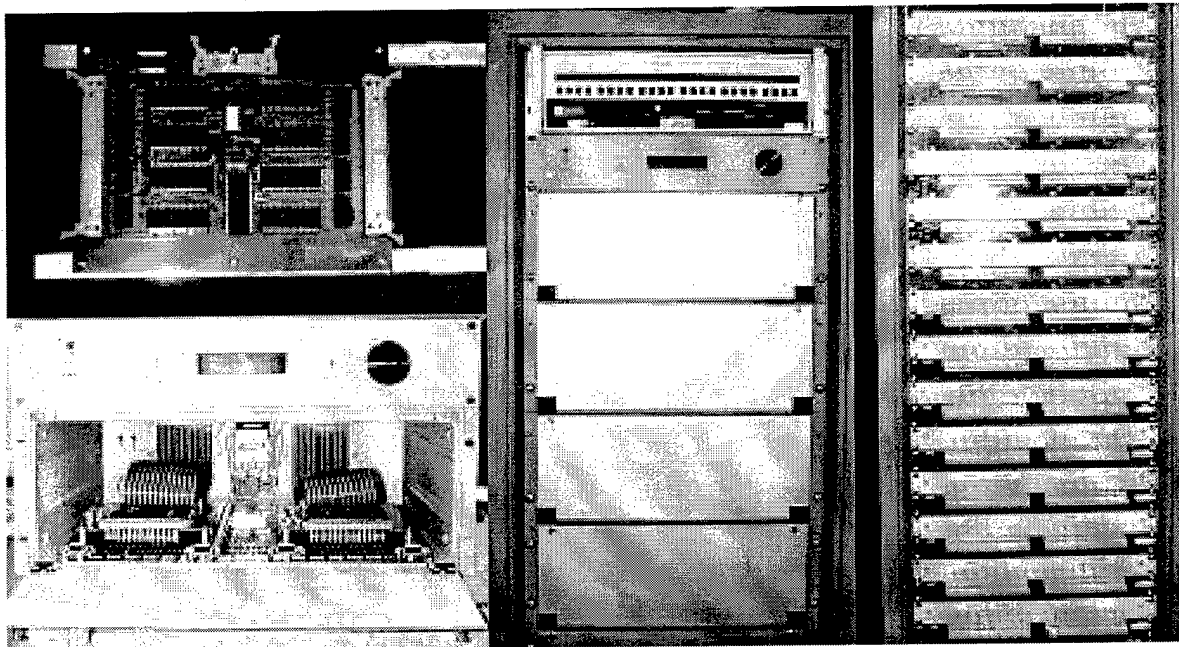


Fig. 10. Data Acquisition System.

The printed circuit cards are connected to the rear panel through ribbon cables. This allows easy

field replacement of the entire card. Two 64-pin ribbon cables connect the 64 differential signals to

the rear of the chassis. On each card, the signals can be shorted to simulate a 0-volt input. Channel 64 is hard-wired to the voltage source. The signal low input can be grounded in order to measure a floating sensor correctly or can remain floating to measure a grounded signal correctly. The cards are mounted on telescoping slides that allow the operator to extend the card to change jumpers when necessary.

The system controller is the device that is used to input and condition the ESP control lines by providing electrical isolation, conversion to 5-v logic level signals, and correction of any transmission delays. An electrically programmed logic device is used to output and retransmit gated, time-corrected channel addresses to the multiplexer chassis. The system controller may be operated in a manual mode to allow the operator to select the channel with a panel-mount encoder and LED display. When this function was not required, the system controller is placed in the remote control mode for data acquisition. The output to the multiplexer address connector is in binary format for proper addressing, but the output to the display is in BCD format for direct channel readout.

5.4 System Performance

The system can be easily relocated where installation and environmental concerns are optimized. It has been constructed using state-of-the-art components and is expected to provide excellent capabilities for years to come. This system provides a new test capability that will help keep the AEDC at the forefront of ground-based aerodynamic testing and also reduces costs to our test customers. Within a period of four months, the total channel capacity was increased from 112 heat gages to over 400. System performance includes:

1. 1600 or more signal leads are isothermally connected in a small area.
2. Local displays show gage status during installation and checkout.
3. Ability to compensate gage installation and wiring problems with on-card jumpers minimizes repair time.

4. Voltage verification to each module is input and recorded during each test data point to ensure system accuracy.

5. Low-level signals to 20 mV are measured with accuracy better than 10 μ v corresponding to approximately ± 0.1 -percent accuracy for typical heat gage signals.

6. Ability to disconnect and relocate in 4 hours.

7. Five installations have been completed to date without system failure.

6.0 Data Productivity and Cost Comparison

The previous Tunnel B/C multiplexing data system was capable of acquiring data from 112 Schmidt-Boelter gages simultaneously. There was no practical way to measure any more sensors without a major equipment and software upgrade. The costs to perform this upgrade were compared to the costs of multiple test entries and the costs were comparable.

An alternative approach was to fabricate a system that would interface the sensor signals to the existing data system using electronically scanned pressure (ESP) control wiring. This effort was approximately one-third the cost of either of the previous two suggestions.

The signal multiplexer system and software revisions conceived, designed, fabricated and successfully implemented resulted in a cost avoidance of \$208,000 for one test program and provided a new data acquisition capability for the AEDC testing complex. Due to the nature of the system construction, it can be used in any AEDC test facility to expand input capability with minor software revisions.

7.0 Summary

Conventional (0.187-in.-diam) and miniature (0.062- and 0.125-in.-diam) Schmidt-Boelter gages were successfully employed to conduct heat-transfer measurements on a complex model covering major portions of both the ascent and descent trajectories of the associated flight vehicle at Mach numbers of 6, 8, and 10. The test model localized

geometry variability and wide range of heat-transfer rate from windward to leeward model surfaces led to the selection of specialized Schmidt-Boelter gages as the sensors of choice. The Schmidt-Boelter gage features simultaneous measurement of both heat flux and temperature to provide heat-transfer coefficient. These gages were fabricated to conform to highly variable local contours with small radii, and where space constraints existed, were fabricated to be less than 0.10 in. in length. These Schmidt-Boelter gages retained the desired sensitivity and provided a NIST-traceable and certified secondary standard.

The requirement of an exceptionally large number of parameters and capability to measure low output signals led to the development of a new robust data acquisition system. The data acquisition system is capable of simultaneous measurement of 400 heat-transfer gages or 800 individual measurement parameters. The capability to obtain measurements for a complete configuration results in a reduction of tunnel run time, higher data productivity, and an overall decrease in the final customer cost (best value) for a program of this scope. The near real-time data turnaround cycle enables the customer to make intelligent decisions with regard to possible changes in the test matrix near real time as the test progresses. This approach proved to be cost-effective and significantly improved the data acquisition capabilities at the AEDC. The system modular design permits future expansion and is inherently transportable.

Acknowledgements

The authors wish to thank the National Space Development Agency of Japan and Mitsubishi Heavy Industries, Ltd. for their permission to use the HOPE model photographs presented in this paper.

References

1. Kidd, C. T., "A Durable, Intermediate Temperature, Direct-Reading Heat-Flux transducer for Measurements in Continuous Wind Tunnels," AEDC-TR-81-19 (AD-A107729), November 1981.
2. Kidd, C. T., "How the Schmidt-Boelter Gage Really Works," Proceedings of the 41st International Instrumentation Symposium, May 1995, pp. 347-368.
3. Strike, W. T., Coulter, S. M., and Mills, M. L., "A 1991 Calibration of the AEDC Hypersonic Wind Tunnels (Nozzle Mach Numbers 6, 8, and 10)," AIAA-92-5092, Dec. 1992.
4. Wannenwetsch, G. D., et. al., "Measurements of Wing-Leading Edge Heating Rates on Wind Tunnel Models Using the Thin-Film Technique," AIAA 20th Thermophysics Conference, June 1985.
5. Kidd, C. T., "Lateral Heat Conduction Effects on Heat-Transfer Measurements with the Thin-Skin Technique," ISA Transactions, Vol. 26, No. 3, July 1987.
6. Trimmer, L. L., Matthews, R. K., and Buchanan, T. D., "Measurement of Aerodynamic Heat Rates at the AEDC von Karman Facility," International Congress on Instrumentation in Aerospace Simulation Facilities, Sept. 1973.
7. Gardon, Robert, "An Instrument for the Direct Measurement of Intense Thermal Radiation," *The Review of Scientific Instruments*, Vol. 24, May 1953, pp. 366-370.
8. Malone, E. W., "Design and Calibration of Thin-Foil Heat Flux Sensors," ISA Transactions, Vol. 7, 1968, pp. 175-179.
9. Kidd, C. T., Nelson, C. G., and Scott, W.T., "Extraneous Thermoelectric EMF Effects Resulting from the Press-Fit Installation of Coaxial Surface Thermocouples in Metal Models," Proceedings of the 40th International Instrumentation Symposium, May 1994, pp. 317-335.
10. Hedlund, E. R., Hill, J. A. F., Ragsdale, W. C., and Voisinet, R. L. P., "Heat Transfer Testing in the NSWC Hypervelocity Wind Tunnel Using Co-Axial Surface Thermocouples," NSWC MP 80-151, March 1980.
11. ASTM Publication: MNL 12, "Manual on the Use of Thermocouples in Temperature Measurement," Fourth Edition, April 1993.

12. Carslaw, H. S. and Jaeger, J. C., *Conduction of Heat in Solids*, Clarendon Press, Oxford, 1959 (Second Edition).
13. Ozisik, M. N., *Boundary Value Problems in Heat Conduction*, International Textbook Company, Scranton, PA, 1968.
14. Kidd, C. T. and Scott, W. T., "New Techniques for Transient Heat Transfer Measurement in Hypersonic Flow at the AEDC," AIAA Paper 99-0823, Jan. 1999.
15. Harms, R. J., et al., "A Manual For Determining Aerodynamic Heating of High - Speed Aircraft," Vol. I, Report No. 7006-3352-001, June 1959, Bell Aircraft Corporation.
16. Kidd, C. T., "High Heat-Flux Measurements and Experimental Calibrations/Characterizations," NASA CP 3161, April 1992, pp. 31-50.
17. Tsai, B. K., Annageri, M. V., and Saunders, R. D., "Radiative Calibration of Heat Flux Sensors at NIST-An Overview," IMECE Technical Paper, Nov. 1997.
18. "Assessment of Wind Tunnel Data Uncertainty," AIAA S-071-1995, 1995.